

Available online at [www.sciencedirect.com](http://www.sciencedirect.com)

ScienceDirect

journal homepage: [www.elsevier.com/locate/jmrt](http://www.elsevier.com/locate/jmrt)

## Review Article

# Current global scenario of Sputter deposited NiTi smart systems



Ajit Behera <sup>a</sup>, Dipen Kumar Rajak <sup>b,\*\*\*</sup>, Reza Kolahchi <sup>c,d</sup>,  
 Maria-Luminița Scutaru <sup>e,\*\*</sup>, Catalin I. Pruncu <sup>f,g,\*</sup>

<sup>a</sup> Department of Metallurgical and Materials Engineering, National Institute of Technology, Rourkela, India

<sup>b</sup> Department of Mechanical Engineering, Sandip Institute of Technology and Research Centre, Nashik, India

<sup>c</sup> Faculty of Civil Engineering, Ton Duc Thang University, Ho Chi Minh City, Viet Nam

<sup>d</sup> Institute of Research and Development, Duy Tan University, Da Nang, Viet Nam

<sup>e</sup> Transilvania University of Braşov, B-dul Eroilor, 29, Braşov 500036, Romania

<sup>f</sup> Department of Mechanical Engineering, Imperial College London, Exhibition Rd., London, UK

<sup>g</sup> Design, Manufacturing & Engineering Management, University of Strathclyde, Glasgow, G1 1XJ, Scotland, UK

## ARTICLE INFO

## Article history:

Received 7 August 2020

Accepted 12 October 2020

Available online 22 October 2020

## Keywords:

Smart metal

Shape memory alloy (SMA)

NiTi

Thin film

Miniaturised system

## ABSTRACT

This review provides details of the global scenario on the recent development and application of NiTi smart metal shape memory alloys (SMA). It mainly focuses on the dc/rf magnetron sputtering fabrication technology of nitinol thin film, which is a prominent structural material for many miniaturised systems. The sputtering parameters and their influence on the smart mechanism of the NiTi thin film has highlighted. The application of NiTi SMA at industrial scale from aviation industries to medical industries was discussed. The raised challenges within various applications were addressed, discussed and we have proposed possible way to overcome these limitations.

Published by Elsevier B.V. This is an open access article under the CC BY-NC-ND license (<http://creativecommons.org/licenses/by-nc-nd/4.0/>).

Abbreviations: a, b, c, lattice constant;  $A_f$ , austenitic temperature; amu, atomic mass unit;  $\alpha$ , angle between b and c; bcc, body-centered-cubic; FIR, Far infrared radiation; hcp, hexagonal close-packed; SMAs, shape memory alloys; M phase, martensite phase (monoclinic structure);  $M_s$ , martensitic finish temperature; MEMS, Micro-Electro-Mechanical System; O phase, orthorhombic phase; R phase, Rhombohedral phase;  $R_s$ , Rhombohedral starting temperature; SME, shape memory effect; PE, Pseudoelasticity.

\* Corresponding author.

\*\* Corresponding author.

\*\*\* Corresponding author.

E-mail addresses: [dipen.pukar@gmail.com](mailto:dipen.pukar@gmail.com) (D.K. Rajak), [luminitascutaru@yahoo.com](mailto:luminitascutaru@yahoo.com) (M.-L. Scutaru), [catalin.pruncu@strath.ac.uk](mailto:catalin.pruncu@strath.ac.uk), [c.pruncu@imperila.ac.uk](mailto:c.pruncu@imperila.ac.uk) (C.I. Pruncu).

<https://doi.org/10.1016/j.jmrt.2020.10.032>

2238-7854/Published by Elsevier B.V. This is an open access article under the CC BY-NC-ND license (<http://creativecommons.org/licenses/by-nc-nd/4.0/>).

## 1. Introduction to smart material

In this advanced material era, the use of smart materials in structural and functional system has an extreme peak in wide range of industries from aviation to medical industries. Smart materials and smart system attracted numerous researchers and technologist due to their extraordinary scientific and technological importance. From past literature, were found other terminologies for smart materials as: intelligent materials, stimulated materials, and responsive materials. These smart materials can better operate in combination of the control unit and are constitutes of the smart system. Generally, a smart system encloses the structural network with macroscopically function with inherent sensing, actuating and controlling capability. It potentially is capable for processing information through its microstructure, also has the distinctive property to reciprocate to its original configuration, through the application of different stimuli such as electric field, magnetic field, electro-magnetic field, temperature, chemicals or stress fields. In the 21st century, the science and technology rely on the evolution of novel smart materials that are expected to react to the environmental changes and manifest their functions according to the optimum conditions [1,2]. The further development of smart materials used in many fields of science and technology for instance in micro-electronics, information science, medical treatment, computer science, life science, transportation, energy, safety engineering as well as in military technologies is paramount important. Now-a-days, the most used materials for intelligent structural applications are the shape memory materials, the piezoelectric materials, electrostrictive materials, magnetostrictive materials, electro-rheological materials, magneto-rheological materials, fiber optics, smart fluid and some functional polymers. In consideration of small-scale actuation, shape memory alloys offer highest actuation force among all other actuation modes like piezoelectric, electrostatic. The smart systems made of shape memory materials employed in different engineering are capable to perform specific activities that are mentioned in following Table 1. Furthermore, to improve the commercial demand as well as to meet the requirement of the hi-tech society, a higher technical and functional standard of SMA activities should be targeted and developed.

## 2. Shape memory alloys

Shape-memory alloys (SMAs) have beneficial properties such as high power-to-weight (or force-to-volume) ratio, pseudoelasticity, higher damping capacity, chemical resistance and biocompatibility [3]. The fundamental phenomenon of the shape recovery based on shape memory effect (SME) and pseudoelasticity (PE) is driven by the phase transition between low temperature (martensite) phase to high temperature (austenite) phase [4]. Both the SME and PE behaviour has shown schematically in Fig. 1 and Fig. 2, respectively. Martensite phase is a low symmetry phase; whereas austenite phase is a high symmetry phase. All the phase transformation which occur in SME and PE are diffusion-less transformation. Due to phase transformation, deformed shape can revert to its original shape when heated above its transition temperature. The phase transformation in SMAs undergoes remarkable changes in the physical, mechanical, chemical, electrical and optical properties, such as surface texture, surface roughness, yield stress, elastic modulus, shape recovery, damping, thermal conductivity, thermal expansion coefficient, electrical resistivity, vapour permeability and dielectric constant, etc. These changes in properties enable designing and fabrication of superior micro-sensors, micro-actuators and so on [4]. In martensitic phase, the material can be easily deformed through twin rearrangement below the martensitic finish temperature ( $M_f$ ). Then, it can revert to its predetermined shape when heated above austenitic finish temperature ( $A_f$ ). This process is a fully reversible phase alteration and reorientation among martensite variants. In this phase transformation, atoms are rearranged with a coordinated fashion by a shear-like self-accommodation mechanism known as the military transformation that arises at the speed of sound in the material [5,6]. According to the response of shape memory materials, there are two types of effect: one-way SME and two-way SME. In one-way SME, the material returns to its initial dimension after heating above the austenitic temperature but does not return to its deformed state when cooled [7]. For two-way SME, a biasing stimulus like a spring effect is required to deform the dimension of the material in the martensitic phase. The growth of SMA in thin film opens broad approach in micro-electro-mechanical-systems (MEMS) and Bio-MEMS. The potential properties with supplementary superelasticity

**Table 1 – Essential inherent activities of shape memory material.**

Activities	Description
Sensing function	Shape memory materials should perceive some specific surrounding changes or stimuli such as thermal, electric field, magnetic field or stress stimuli
Switching	The change in surroundings must reach a predetermined value to start/restart the inherent performance
Actuation function	Shape memory materials yield substantial displacements with switching performance with prodigious forces for actuation
Repeatability	The shape recovery or other changes are capable of reversing and can be recapitulating for a more substantial number of cycles
Energy cache and transformation	A significant amount of energy can be cache, and energy conversions such as thermal-mechanical, electric-mechanical, magnetic-mechanical and chemical-mechanical may be executed

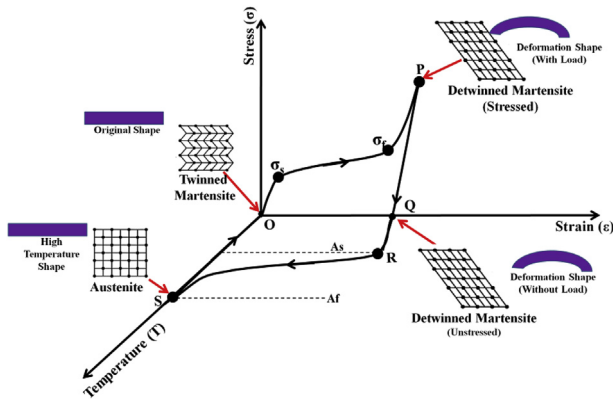


**Fig. 1 – Schematics of (a) stress–strain–temperature ( $\sigma$ - $\epsilon$ - $T$ ) for SME curve associated with temperature induced shape memory alloys.** The original shape i.e. low temperature shape is twinned martensite at “O” subjected to loading (stress) and follow O  $\rightarrow$  P path. When the twinned martensite is subjected to an applied stress which exceeds the start stress level ( $\sigma_s$ ), the reorientation process begins, causing the growth of certain favourably oriented martensitic variants which develop at the expense of other less favourable variants. The detwinning process is completed at a stress level,  $\sigma_f$ , that is characterized by the end of the plateau in the  $\sigma$ - $\epsilon$  diagram. At the point of unloading at “P”, it follows P  $\rightarrow$  Q path and the detwinned martensitic is preserved. There is a requirement of external stimuli for recovery. When heating in the absence of stress, the reverse transformation begins when the temperature reaches  $A_s$ , (in R) and ends at the temperature  $A_f$  (point S), above which only the original austenitic phase exists. In the absence of permanent plastic strain generated during detwinning, the original form of the SMA is recovered. The strain recovered due to the phase transformation of the detwinned martensite into austenite is called the transformation strain.

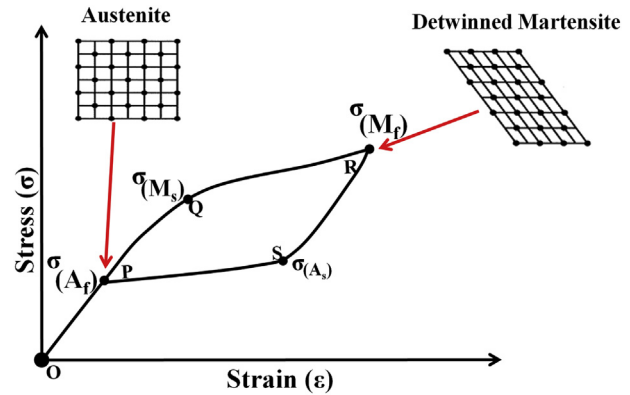


**Fig. 2 – Stress induced phase transformation, i.e. stress–strain ( $\sigma$ - $\epsilon$ ) curve of pseudoelasticity (PE).** PE property allows SMAs to withstand large amounts of stress without undergoing permanent deformation. The transformation occurs without temperature change. The SMA temperature is maintained above the transition temperature. The stress increases until the austenite becomes martensitic. The result of this loading is a fully detwinned martensite created from austenite. When the load is reduced, the martensitic transformations return to austenite. The SMA returns to its original form because the temperature is always higher than the transition temperature. This is a consequence of a stress-induced transformation from austenite to martensite and vice versa.

and biocompatibility have shown a great interest in NiTi-based SMAs for functional applications at low (e.g., Ni–Ti  $< 100$  °C) temperature as well as at high (e.g., Ni–Ti–Hf  $> 100$  °C) temperature.

### 3. NiTi shape memory alloys

NiTi alloys were used as SMAs for more than three decades in the form of actuators, couplings, fasteners, and connectors in a wide area from automotive and aerospace industries medical industries. Commercial based equiatomic NiTi SMAs are known for over 35 years, and the NiTi thin film used in MEMS is known for about a decade. A large variety of alloys exhibits shape memory effect (SME), but small numbers of alloys like NiTi have received commercial exploitation. Hexagonal close-packed Ti undergoes polymorphic change at high temperature to body-centered-cubic phase, limits the Ni solubility ( $< 10$  wt % Ni at 942 °C). NiTi-based SMAs have drawn researchers' attention for actuators, which operate with large stress and

strain and possesses impressive properties like shape memory effect (SME), superelasticity (SE), high damping capacity, high specific energy output, biocompatibility, and high corrosion resistance. By heating or loading, the dimensional recovery of the intermetallic alloy possesses a reversible thermo-elastic phase transformation restricting the long-range diffusion [8]. Shape memory alloys are able to transform from the parent phase (austenite phase, B2 phase, BCC crystal structure), to martensitic phase (B19' phase, monoclinic crystal structure) just above room temperature. This transformation may occur through metastable intermediate R-phases in case of Ni-rich NiTi alloys. The phase transformation associated with the diffusionless shear dominant process retain their same chemical composition for the parent and product phases [9]. In the phase transformation process, there is a perceptible surface relief, and a flat surface at high temperature (austenite phase) changes to rough (twinned martensite) when achieving the lower temperature, and vice versa. The change in surface roughness during the thermal cycle is related to the phase transformation that advances with both the grain growth and the orientation [5,10]. The key element enabling the functioning of SMAs is linked to the transformation temperature and percentage of recover-strain. This is greatly influenced by the composition and thermal treatment of the materials. Ni–Ti alloys are contain some diverse phases (e.g., B2, B19, B19', and R phase) and different twin structure (e.g., Type-I, Type-II, and compound twin). The

transformation temperature and shape memory characteristics of NiTi SMAs depends on metallurgical factors such as alloy composition, annealing temperature, aging temperature, aging time and substrate temperature and processing parameters (i.e. sputtering parameters: current, voltage, primary gas flow rate, carrier gas flow rate, substrate bias etc.) [11]. These factors drive the physical, mechanical, chemical, electrical as well as their optical properties. The structural composition Ni and Ti element were outlined in Table 2.

#### 4. NiTi thin film SMAs

The NiTi SMA thin films are favourable candidate for micro-electro-mechanical-systems due to its large work energy densities, low power consumption, unique SME property, long lifetime and good response to batch-processing technology of silicon micromachining [4,15,16,17]. They have also excellent resistance to corrosion and biocompatibility of SMAs leading to the development of exciting biomedical parts, including stents, tissue fixation (ISO.25217), and drug delivery, etc. [18–25]. The composition for optimum shape memory effect in a film can differ from that of the bulk alloys, which are influenced by grain sizes, plane stress conditions and surface effects [26]. The bulk SMAs manifest large strokes and forces but experience a slow response, because SMAs are typically thermally actuated. The way of heat supply and removal in a cycle is directly influenced by the cycle-time, which is a sensitive parameter. As a comparison to bulk SMAs, thin films yield enables faster cooling rate due to their high surface-to-volume ratio, increasing the rate of heat transfer and, hence, the cycle-time can be decreased. It is found that NiTi shows the larger strain recovery and stress recovery that is up to 6–8% and 600 MPa, respectively. It is much larger as compared to other actuation materials like electrostatic and piezoelectric materials. The higher strain recovery integrated with a higher stress recovery results in a larger work density, up to

$2.5 \times 10^7 \text{ J/m}^3$  [3,21,27,28]. To increase the response of NiTi thin film SMA microactuators, it is imperative to decrease the cycle-time, i.e., the time required for the transformation between austenite and martensite during cooling. Reduction of cycle time is possible by (a) improving the rate of cooling in thin film SMAs, and (b) minimizing the temperature range of heating cooling to complete the transformation in forward and reverse direction [29]. The thin film is efficiently driven by joule energy during electrical heating and triggers the faster cooling rates [2,15,30,31]. The uniformity composition of thin film across the surface is a very significant factor for the thin film SMA synthesis which is regulates by deposition geometry (i.e. substrate to target distance, target diameter, the angle of target, etc.) and type of target used (i.e., elemental, alloy, or mosaic structure, etc.) [32–34]. The most critical requirements for enabling the technologies of NiTi thin films include [4,35–37]:

- (i) Economic, user-friendly, safe, infallible and MEMS suited synthesis technique; accurate composition control of the thin film and their quality.
- (ii) Noiseless and silent working due to the characteristic microstructures and phase transitions.
- (iii) Real-time response (the materials can respond as soon as to the sense of stimuli)
- (iv) High actuation speed and fast response.
- (v) The feasibility of nano size Ni–Ti structured thin films and actuators.
- (vi) Less defect and less residual stress to obstruct any inconvenience with MEMS structure, and better adhesion to the substrate.
- (vii) A predefined annealing or ageing process after deposition for film crystallization, which will well match with the MEMS process.
- (viii) An appropriate characterization for PE, SME, and their mechanical properties.
- (ix) Wide range of operational temperatures.

**Table 2 – The structural composition of Ni and Ti element [5–14].**

Atomic Parameters	Ni	Ti
Atomic Number	28	22
Atomic mass	58.6934 amu	47.867 amu
No. of proton/electron	28	22
No. of neutron	31	26
Group, period, block	Group-10, period-4, d-block	Group-4, period-4, d-block
Melting point	1453 °C	1660 °C
Boiling point	2732 °C	3287 °C
Crystal structure	Cubic (FCC)	Hexagonal (HCP)
Density (at room temperature)	8.908 g/cm <sup>3</sup>	4.506 g/cm <sup>3</sup>
Colour	White	Silver
Electronic configuration	[Ar]4s <sup>2</sup> d <sup>8</sup> or [Ar]4s <sup>1</sup> 3d <sup>9</sup>	[Ar]3d <sup>2</sup> 4s <sup>2</sup>
Heat of fusion	17.48 kJ/mol	14.15 kJ/mol
Heat of vapourization	377.5 kJ/mol	425 kJ/mol
Molar heat capacity	26.07 J/mol.K	25.060 J/mol.K
Electronegativity (pauling scale)	1.91	1.54
Atomic radius	124 pm	147 pm
Electrical resistance (20 °C)	69.3	420 nΩ
Thermal conductivity	90.9 W/mK	21.9 W/mK
Thermal expansion (25 °C)	13.4 μm/m.K	8.6 μm/m.K
Magnetic ordering	Ferromagnetic	paramagnetic

- (x) Good surface wear and corrosion resistance properties.
- (xi) Greater biocompatibility in application towards bio-MEMS.
- (xii) Possess higher ingrained specific damping capacity
- (xiii) Better embeddability and reliability.

Currently, the global SMA market size progressing with compound annual growth rate of 10.79% and predicted to reach USD 11,079.1 million by 2023. Miniaturized equipment assisted NiTi thin film has taken a dominant segment in the market demand. Global NiTi SMA market include constantly growing usage of SMA for medical and clinical industries, electronic industries, energy harvesting industries, and household decorative. On the basis of the application, the NiTi thin film market is segmented into superelastic, actuators, constrained recovery, frangible, vibration dampers, shock absorbers, and others, as shown in Fig. 3. Some of the key players operating in the global NiTi thin film SMA market are SAES Getters S.p.A, Ultimate NiTi Technologies Inc, Endo-smart GmbH, TiNi Alloy Co, Fort Wayne Metals Inc., TiNi Aerospace, DYNALLOY Inc., Metalwerks PMD Inc, EUROFLEX GmbH, Inc, AeroFits Products Inc, Admedes Schuessler GmbH, Johnson Matthey Inc, Furukawa Electric Co. Ltd, Confluent Medical Technologies, Baoji Seabird Metals Materials Co. Ltd., Burpee Materials Technology LLC., and Baoji Titanium Industry Co. Ltd.

## 5. Development of NiTi thin film using magnetron sputtering

By the envision implementation for MEMS, the different approach was attempted for the synthesis of NiTi thin films. From the experimental viewpoint, only the magnetron sputter technique has superseded in the deposition to give a faultless SME behaviour in the thin film as comparison to that of bulk materials [3]. In the sputtering process, atoms sputtered from the target material by the carrier gas (Ar, N<sub>2</sub>, etc.) and condense onto various substrates to develop a thin film. Phase transformation temperatures, SME and PE behaviour of sputtering deposited NiTi thin films are sensitive to metallurgical factors (percentage of composition in alloy, pre- and post-thermo-mechanical treatments, etc.), sputtering target arrangement (co-sputtering, mosaic deposition, and alternative layer deposition etc.), sputtering parameters (targets material purity, target power, flow rate of primary and secondary gas, substrate-to-target distance, substrate

temperature, substrate bias, and the deposition environment etc.), and also sensitive to predetermined application conditions (stress and strain rate, loading conditions, heat removal, rate of heating/cooling, etc.) [4]. If Ni<sub>50</sub>Ti<sub>50</sub> alloy target is used in sputtering, the compositions of the final deposited thin films are always Ni-rich, because the sputtering yield for Ti is lower than that of Ni [3]. It was found that equiatomic NiTi target gives Ti poor thin film regarding the target by 2–4 at %. The sputter yield can be measured by the ratio of the number of atoms ejected from the target to the number of the atoms incident to the target. The inherent difficulties associated with sputtering of NiTi thin films include the dissimilar sputtering yields of elements at a given power density, compositional uniformity on the substrate surface and along the interface, in addition to wear, and roughening of the target during sputtering. To avoid the sputter yield difficulties, co-sputtering of the NiTi target with additional Ti target, or using two separate single elements (Ni and Ti) targets, with another small Ti plates on NiTi target is used. The film composition from different targets, managed by the power ratio, is more reliable to overcome the composition control difficulties [32]. Rotation of the substrate during deposition, configuring and positioning the target, etc. are also helpful. A trace amount of impurities (typically C, O<sub>2</sub>, and H<sub>2</sub>) can increase the brittleness and decreases the SME behaviour. For this reason, it is essential to set the purity of carrier gas and target and to fix the chamber vacuum at high nearly 10<sup>-6</sup> Torr. Before deposition, pre-sputtering should be necessary to rinse the target surface, ensuring about the removal of surface oxides. The quality of film also influences by the environmental conditions inside the deposition chamber. Too low and too high working pressure is not a desirable quality of the thin film. So ultra-high purity primary gas with working pressures ranging from 0.1 to 0.93 Pa (0.75–7 mTorr) is preferable. The substrate-to-target distance should be optimized which directly affects the particle energy reaching at the substrate as well as the composition uniformity of the thin film [38]. Film composition shifts can experience due to sputtering yield differences, angular flux distribution, velocity distribution, and lateral diffusion of the sputtered species due to atomic collisions among gasses [39,40]. During sputtering, 95% of the energy goes into the target during the incident, and only 5% of incident energy is brought off by target atoms (the typical energy of 5–100 eV). Ni and Ti adatoms acquire a high-temperature state before reaching the surface of the substrate. When these adatoms deposited on the surface, the substrate act as a heat sink and it takes around to be on the order of 10<sup>-12</sup> s to come to its energetically equilibrate state. It is estimated that an atom with a 0.1 eV energy is comparable to a temperature of 1000 °C and it deposited with a quenching rate is of approximately 10<sup>15</sup> °C/s [41]. This higher cooling rate usually allows non-equilibrium atomic arrangements in the thin film unlike the bulk thermodynamic criteria [42,43]. This non-equilibrium processing state arises by incorporation of the elements having zero solid–liquid solubilities and such non-equilibrium films in higher annealing temperature transforms into the equilibrium phases.

In sputter deposition, the different type of target such as elemental form, alloy form and mosaic-structured target can be used [44–46]. Successful execution of NiTi microactuators

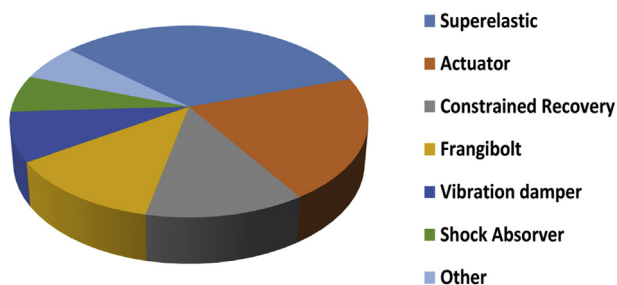


Fig. 3 – Global market size of NiTi thin film.

needs a better interpretation of the sputtering process of NiTi thin films and their final microstructure. During sputtering deposition of NiTi thin film, a few disadvantages has reported: (1) It is not easy to get the exact chemical composition of sputtered NiTi thin film with that of the target alloy used., (2) There is a high chance of oxidation of Titanium. Hence vacuum chamber with inert gas purging is required [47], (3) Contamination during the sputtering/resputtering process by the substrate surface [47].

### 7. Ni–Ti phase diagram and its significance

The phase diagram of NiTi gives the link between the transformation temperature, compositions, microstructure, and the development of precipitates [48]. There are three ways of phase transformation in different NiTi based thin films: (1) B2 phase (parent phase, cubic structure) → B19' phase (martensite phase, M phase, monoclinic structure); (2) B2 phase → R-phase (Rhombohedral phase) → B19'; and (3) B2 phase → B19 (O phase, orthorhombic structure) → B19'. Compositional sensitivity for different phase transformation is due to the presence of the restricted intermetallic area in the Ni–Ti Phase diagram (Fig. 4) [49].

The film composition, annealing and ageing treatments of the thin film are the factors mostly affect the transformation temperatures [33,50]. The NiTi phase diagram indicates the Ti solubility in Ni–Ti alloy that may affect the transformation temperatures [51]. Direct transformation of the B2 phase to the B19' phase occurs in crystallized binary NiTi alloys. Two-step transformation B2 to B19' phase via R-Phase occurs in case of thermomechanical treatments, thermal cycling, or by the addition of a third alloying element (ISO.25217) [18–25,52]. The B2 structure of NiTi alloys is CsCl-type having a lattice

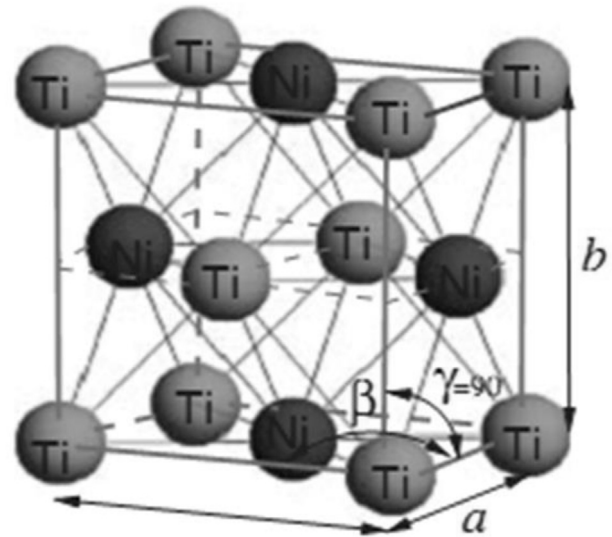


Fig. 5 – B2 structure [54].

constant of 0.3010–0.3020 nm [53]. The B2 phase crystal structure is given in Fig. 5[54]. The transformation between B2-phase to R-phase is important in actuator applications because it is interconnected with less hysteresis loop than that of B2 to B19' transformation [31,55]. For NiTi, the transformation of B2→R-phase occurs during heat removal at a temperature  $R_s$ , at which the B2 phase is distorted in the  $\langle 111 \rangle$  direction to produce R-phase, depicted in Fig. 6[56].

The R-phase having lattice constants are  $a_h = 7.3580 \text{ \AA}$  and  $c_h = 5.2855 \text{ \AA}$ , which deviates by 1.4% and 2.4%, respectively, from the calculated value [9]. Strain and the hysteresis range of R-phase transformation was nearly

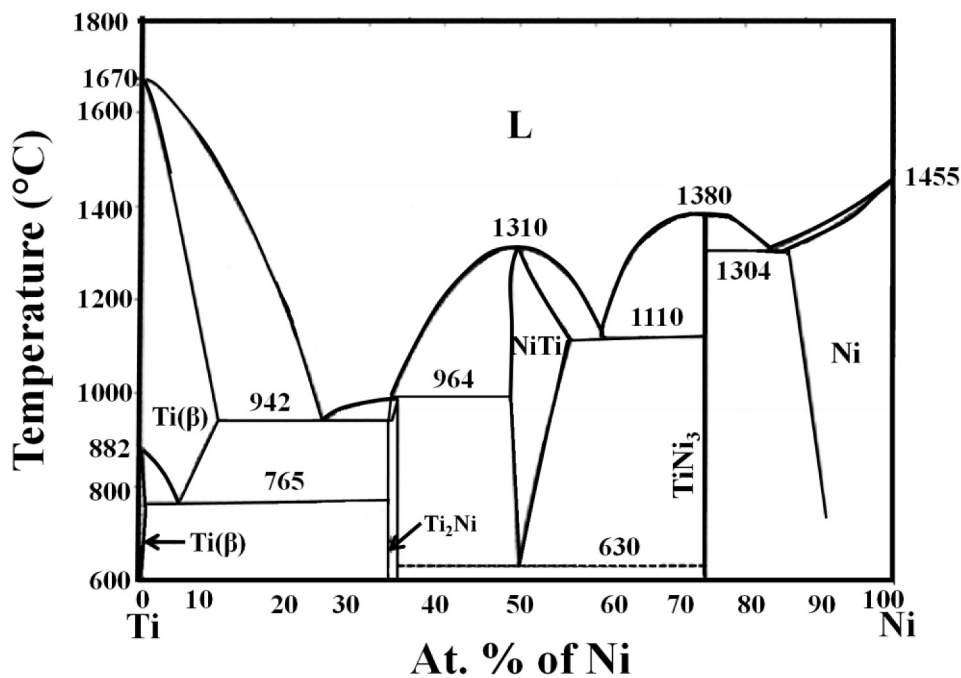


Fig. 4 – NiTi phase diagram.

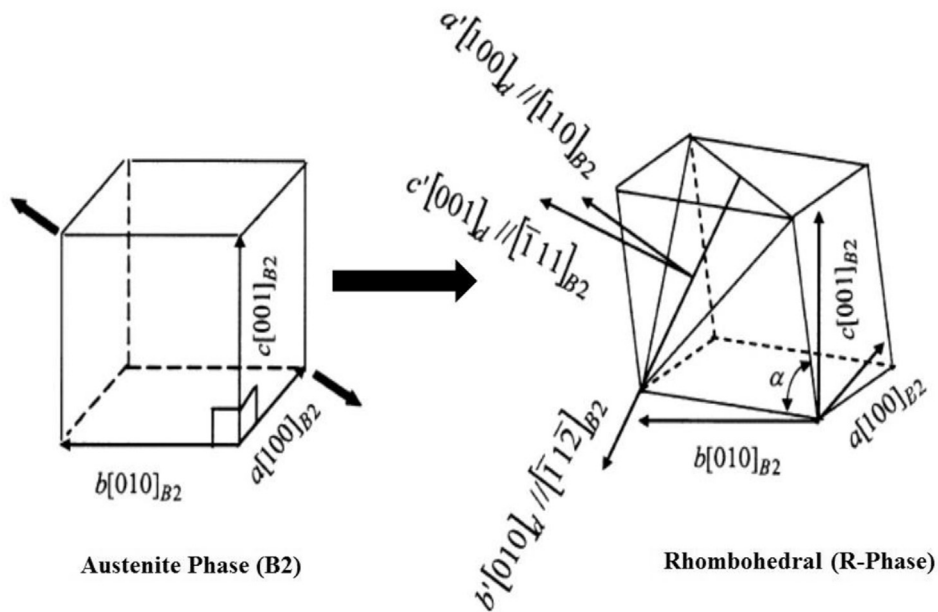


Fig. 6 – Transformation of B2-phase to R-phase [56].

one-tenth of austenite to martensite phase transformation [57]. The lattice constants ( $a$ ,  $b$ , and  $c$ ) changes during austenite to martensite transformation are 27.0%, 8.8%, and 21.6%, respectively, whereas the unit lattice volume change only by 0.4%. The B19' structure (Fig. 7) has lower symmetry than B2 [54]. The R-phase has some attractive properties such as stability at a higher number of thermal cycling with its quasi-reversible transformation and negligible strain-recovery fatigue. Therefore, the R-phase transformation is the most suitable transformation for quicker response and can be used in a high-speed micro-actuator [58,59]. The stability of R-phase is more because, in phase conversion, the strain is so small that slip deformation hardly occurs [60].

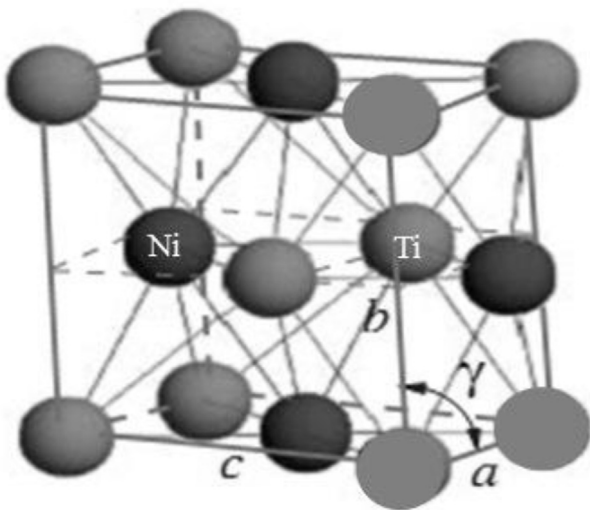


Fig. 7 – B19' structure [54].

## 8. Effect of intermetallics in NiTi alloys

The as-received NiTi thin film is an amorphous structure, which undergoes annealing treatment for achieving the crystalline structure that requires exhibiting the better shape memory effect. During crystallization kept attention needed for avoiding the formation of intermetallic and the chemical interactions between the substrate and the deposited phase that deteriorate the SME and PE characteristics of the thin film. The typical crystallization temperatures range for NiTi alloys are 723–973 K. The formation of intermetallic cannot avoid with 300 °C annealing temperature. Annealing temperature above 823 K with higher annealing time generates the intermetallics of NiTi<sub>2</sub>, Ni<sub>4</sub>Ti<sub>3</sub>, and Ni<sub>14</sub>Ti<sub>11</sub> in the form of precipitates [61]. Different precipitates and finer grain may seize the martensitic transformation [62,63]. Generally, by annealing, Ni<sub>4</sub>Ti<sub>3</sub> phase forms in Ni-rich thin films and NiTi<sub>2</sub> phase forms in Ti-rich thin film [64]. It is found that the crystal structure of NiTi<sub>2</sub> is FCC with a lattice parameter four times larger than that of NiTi [65]. During the transformation from amorphous to crystalline, the NiTi<sub>2</sub> nucleates and grows along the grain boundaries of austenite due to the higher concentration of Ti in Ti-rich thin film [63,66]. The growth of NiTi<sub>2</sub> precipitates is uncontrollable which can disturb or impede the growth of martensite plates [11,67]. The Ni<sub>4</sub>Ti<sub>3</sub> precipitates in the thin film favour the phase hardening by ceasing the movement of dislocations and suppress the martensitic transformations. The phase hardening tendency of precipitate in an alloy decreases as the heat-treatment temperature increases and it exhibits thermoelastic martensitic transformation [68]. The crystal structure of the Ni<sub>4</sub>Ti<sub>3</sub> precipitates has a unit cell having lattice parameters,  $a = 0.670$  nm,  $\alpha = 113.8^\circ$ . [69–71]. The main advantages of NiTi intermetallic are: excellent mechanical properties and stability, good

corrosion resistance, superior damping capacity, and higher biocompatibility.

## 9. Some aspects influencing the quality of the NiTi thin film

### 9.1. Argon gas pressure and substrate-to-target distance

The Argon pressure and the substrate-to-target distance suggest the energy carried out by adatoms coming to the substrate. The energy content of the adatom indicates the deposition efficiency, structural integrity, film density, and stress. For higher Ar pressure, thin film results in low density with structural defects whereas, for low Ar pressures, the thin film results denser with fewer structural defects [32]. At very low working pressures, the atoms arrive at the substrate surface having higher energies causes “atomic peening”. By atomic peening, the surface atoms are pressed into the thin film that increase the density and generate the compressive stresses. By gradual increase in gas pressure, there is increasing in adatom momentum in the substrate, the peening effect will cease, the film becomes less dense, and there is a decrease in compressive stress. Further increase in gas pressure results decrease in film density and increase in intrinsic tensile stresses. At higher gas pressure, there are a large number of collisions occurs, the energy of sputter atom decreases, and adatoms coming with low surface mobilities grows in a columnar fashion in thin film. The columnar type of growth has a very low density between the columns gives a reduction of tensile stress. With higher pressure (6.7–13.3 Pa), the films give a porous film along with poor ductility.

In the sputtering deposition, at low gas pressure or small substrate-to-target distance has an intrinsic compressive stress, which converts to tensile with the increase in pressure, becomes maximum at some critical pressure and decreases with further increase in pressure [28]. The thin films processed at high Ar pressure more than 1 Pa give a brittle structure, formation of a crack on the surface, porous structure, delamination at the interface, and biaxial tensile stresses [72,73]. At the higher Ar gas pressure, the columnar microstructure indicates to the larger grains which are developed due to lack of surface diffusion and lack of mobility of adatoms during growth of the film [32]. With higher working pressures, there may be the absorption of Ar atoms in thin film surface which plays a significant role to obstruct the surface diffusion and results in columnar sputtered thin film [28]. At lower Ar Pressure 0.67 Pa (5 mTorr), there is a decrease in adhesion strength between Ti and the Si-substrate in NiTi thin film and increases at higher Ar pressure up to 12.67 Pa (20 mTorr). The adhesion strength in Si and Ti decreases as the film stress in greater than Si–Ti binding strength. Again, with higher Ar pressure, each adatom sit on the substrate surface with less energy and results in lesser film stress. The film stress varies concerning the Ar pressure is directly related with the crystalline structure of the thin film and their orientation and density [74].

### 9.2. Substrate temperature

Higher substrate temperature leads to lower the cooling rate and higher diffusivities of Ni and Ti which results in partial crystallization in the film. At lower substrate temperature, the film gives a continuous network with homogeneously distributed grain boundary like structures. This surface morphology is due to the lack of surface migration by lower energy adatoms which results from inter-columnar porous boundaries. At higher substrate temperature, the surface diffusion of adatoms increases resulting a dense film. A small number of higher energy adatoms makes the grain more elevated in comparison to their neighbouring grain, which contributes to reducing the density of grain boundary [75]. The substrate temperature is restricted up to 300 °C to avoid substrate atom diffusion towards the thin film [76].

### 9.3. Substrate surface roughness

Substrate surface roughness is a dominant parameter that affect the adhesion strength as well as the crystallization temperature of the thin film. By increasing the smoothness of the substrate surface, there would be a decrease in adhesion strength between the substrate and thin film associated to a higher chance of delamination. Hence, increasing the substrate surface roughness leads to an increase in adhesion as well as an increase in the crystallization temperature of the thin film (typically, increment is as high as about 300 °C). However, the crystallization temperature of the thin film is greater than the thick film. Therefore, for quality NiTi thin films, the substrate surface roughness cannot be too smooth or too rough [77].

### 9.4. Film thickness

The film thickness parameter has a great impact on the shape memory effect, transformation temperature, residual strain and mechanical behaviour of thin films. The transformation temperatures are very sensitive to the thickness of the thin film (not more than two micron), residual strain and surface oxidation [33]. For better shape memory behaviour, it will require restricting the thickness of thin film less than 10 µm [78]. Gordon et al. pointed out that the substrate tends to reduce the SME behaviour by decreasing the thickness below a threshold level which is specific to the applied load [79].

### 9.5. Composition variation

The NiTi thin film properties are susceptible to its composition. A minute deviation (<1% of Ni or Ti) from the equiatomic NiTi can significantly change the transformation temperatures. Only 1% change in composition can result in 100 °C shift in transformation temperatures [80]. The composition of the thin film can be controlled by controlling the power ratio of targets. Another factor is composition uniformity across the cross-section, which can be controlled by deposition geometry: size of the target, the shape of targets (single element surface or alloy surface or mosaic surface), the angle of inclination of targets, optimizing the distance between target and substrate, etc. For example, a little deviation of the substrate-

holder from the horizontal plane gives around 1% variation across the 100 mm substrate holder having a diameter of 0.01%/mm [3].

### 9.6. Deposition rate

At low deposition rate, atoms are coming towards substrate have sufficient time to change to low energy state before they are trapped by subsequently deposited atoms results in lower intrinsic stress and smooth surface [19]. The high deposition rate may cause intercolumnar voids.

### 9.7. Stress

Stress in the film surface/substrate and the presence of the interface reaction products, mostly affect the film adhesion. The main causes responsible for the stress evolution in the as-deposited amorphous thin film are (a) mismatch of the thermal expansion in between the substrate and NiTi thin film, (b) the density difference between crystalline and amorphous Ni–Ti thin film [81]. The stresses in the constraint thin films are of three types, i.e., intrinsic stress, thermal stress and phase transformation stress [82]. Both the tensile or compressive residual stress was developed in the sputtered thin films. High residual tensile stress results in film decohesion and film cracking whereas high residual compressive stress results in film delamination and buckling. Post-deposition thermo-mechanical treatment has great significance with the reduction of residual stress [4]. The essential parameters responsible to decrease the residual stress in NiTi thin film are: (a) sharp restriction of the Ni/Ti ratio, (b) deposition of thin film at optimum working pressure, (c) selection of appropriate deposition temperature, in agreement with the development of minimum intrinsic stress and thermal stress, (d) application of intermediate layer to decrease the residual stress in some NiTi thin films., (e) implementing post-annealing such as laser treatment, ion beam post-modification, or in-situ ion beam modification after sputtering to reduce intrinsic stress and (f) selection of appropriate substrate to decrease the thermal stress.

---

## 10. Mechanical properties of the Ni–Ti thin film

### 10.1. Stress–strain analyses

Yield stress, fracture stress, and ductility can be measured using stress–strain curve at different temperature. In Ni50Ti50 thin film, the calculated maximum elongation is greater than 40% [82]. NiTi alloy presents 50–60% elongation and tensile strength as high as 1000 MPa [83]. The martensite phase shows higher yield stress and fracture stress that were more than 600 MPa and 800 MPa, respectively. These mechanical properties show good support about sputter deposited NiTi thin films possessing sufficient ductility and stable SME behaviour for practical applications [82].

### 10.2. Fatigue properties

Fatigue behaviour mostly affects the NiTi thin films after about  $10^6$  cycle that leads to reduce the SME properties. Recapitulating the phase changes will customize the microstructure and transformation hysteresis which give rise to changes in transformation temperatures, transformation stresses, and transformation strains. The fatigue behaviour and the performance degradation of the thin film are affected by interrelated internal parameters (film/substrate interface, lattice structure, alloy composition, defects, and precipitation) and external parameters (thermo-mechanical treatment, applied maximum stress, stress, and strain rate). Fu et al. studied the constrained NiTi thin films fatigue behaviour and reported about the changes of recovery stress during cycling. He observed that the recovery stress of thin film (by curvature measurement) decreased mainly in the first tens of numbers of the cycles and began to be stable after thousand numbers of cycles [4]. This decrease in recovery stress is due to the formation of void, dislocation movement, partial debonding at the interface, grain boundary sliding, non-recoverable plastic deformation, etc.

---

## 11. Tribological properties of NiTi thin film

Surface modifications should be essential for better resistance to wear that required for miniaturized systems and biomedical applications, such as micro-channel, micro-valves, micro-pumps, micro-tweezer, micro-grippers, etc. It was found that cubic austenite phase of NiTi bulk alloys demonstrate an excellent wear resistance due to their pseudoelastic behaviour and rapid work hardening [84] whereas B19' martensite phase shows a poor wear resistance with a higher coefficient of friction. In tribology application of NiTi thin films, large potential stress, a large coefficient of friction, and interfacial adhesion are other crucial analyse [85,86]. NiTi alloys exhibit better erosion resistance than other structural elements due to their pseudoelastic behaviour. Another way to get better surface property is to develop multi-layer, or functionally graded Ni Ti thin film [87,88]. The material properties could change from PE to SME, by changing the content of Ni and Ti in the micrometer-thick film. The assimilation of PE with SME behaviour cause a two-way reversible actuation due to variations of residual stress in the thickness will permit the biasing force to be developed inside the thin film. Another way is the deposition of adherent and hard TiN layer ( $\approx 300$  nm) on NiTi thin film to develop a good passivation layer that increases tribological properties without disturbing the SME [35,89]. To develop adhesion as well as biocompatibility factor, a functionally graded Ti/TiNi/TiN/Si layer can be used. Ti thin layer can obstruct the release of Ni atom (Ni is toxic) with improving the film adhesion. Treatment of NiTi thin films by electrons, ions, and the laser beam has been carried out to improve the surface profile, mechanical strength, corrosion and biological properties for implementation in adverse and wear environment [90–92].

## 12. Multilayered NiTi thin film

Investigation on the field of SMA thin films has achieved an unquestionable degree of maturity [93]. The attention shifts towards a double layer/multiple layer SMA thin films which provide physical and mechanical stability, chemical compatibility, dynamical coupling, and durability. Interface profile (phase gradient, inter-diffusion, interface width, etc.) of the multi-layered thin film is an important factor to fabricate the NiTi multilayered thin film. The phase transformation behaviour concerning coupling components interfaces, including transformation hysteresis, ageing, and phase stability are not well understood so far [61]. Diffusion at different temperature has a vital role in changing the chemical composition of the top layer during sputtering. Ken et al. found that the multilayer structure disappears after annealing at 600 or 873 K for 1.8 ks. In the film, Ni and Ti grains are preferentially oriented in the [111] direction and [002] direction respectively [40,94].

Multilayer deposition has been successfully applied to the fabrication of neutron optical components and X-ray optics as a mirror where very good thickness uniformity of the individual layers and good reproducibility on large substrates were demonstrated [95–99]. The layer-by-layer assembly has gained powerful, flexible and simple thin-film material deposition process with applications spanning surface engineering, photonics, drug delivery, energy and so forth [6–8]. It has been focused most research efforts on novel material assemblies, novel applications of existing material assemblies and understanding the fundamental thermodynamic and transport phenomenon, and there has been substantial work on making the process more rapid, scalable and ultimately manufacturable [100–104].

Some advantages have concluded, comparing multi-layer with the single layer deposited thin film are:

- Multilayer has better hardness and ductility
- There is an increase in cohesion strength between the substrate and multilayer thin film.
- A multilayered thin film with restricted thickness has equal or higher mechanical stability with each of the single constituting layer
- There is lesser in residual stress in multilayer thin films
- The denser structure found out in the multilayer
- By annealing, the multilayers were able to create NiTi homogenized phase throughout the cross-section results a better SME [94].
- Composition control of the final NiTi thin film is easier by controlling the thickness ratio of each layer [94].
- Good magnetic, superconducting properties as compared to single layer thin film

## 13. Industrial applications of NiTi thin film

In micro-electro-mechanical systems, there is a requirement of the assimilation of sensors, actuators and electronic control unit on a Silicon substrate, which has potential compatibility

with batch processing Si micro-fabrication technology. Now-a-days there is a great demand for making micro-machines and micro-robots in a variety of fields such as medicine, biotechnology, electronics, and other industrial fields. The NiTi thin film SMA are the potential candidates for micro-actuators which could be applied to fabricate such type of micro-machine (micro-fluid pumps, micro-valves, etc.) [105,106]. The major aspects are considered to include sputter deposited NiTi thin film into a Si micromachining processes are:

- Better harmony of the thin film with higher annealing temperature;
- A good rapport of patterning techniques for NiTi thin films;
- The specific procedure for releasing the NiTi film from the substrate.

Incorporation of NiTi thin film SMAs in Si micro-machining process was first pointed out in the year 1990 [107]. The manufacturing technique of valve-actuator first developed in NiTi Alloy Company explained in Fig. 8. Micro-actuators entail with substantial recovery stress and large transformation deformation along with high frequency and fast response (less transformation hysteresis). Always there is a challenge to reduce the hysteresis and increase the operating frequency for the wealthy application of NiTi thin films. R-phase transformation in the thin film actuator gives a precise hysteresis temperature, which is essential for the micro-electro-mechanical thin film. In micro-actuator, generation or absorption of heat and dissipation of heat is the key parameters for actuation of the system. By decreasing the amplitude of the cyclic temperature and increasing the working stress, the hysteresis could be slightly minimized. A substrate having a greater coefficient of thermal expansion than the NiTi thin film gives larger compressive stress, which results in a smaller hysteresis. During deposition, all the above key parameters will be counted on the different substrate such as glass, poly-Si, Si<sub>3</sub>N<sub>4</sub>, etc. for successful micro-electro-mechanical applications [108,109]. The behaviour of thin film SMA and established a promising application in graphical mode is represented in Fig. 9[110].

### 13.1. Actuator

A temperature-controlled actuator is operated similar to that of bimetallic effect. Two type of material having a different thermal expansion sandwiched for deflection according to the increasing or decreasing the temperature. Thermostat valve and safety switches are thermal controlled actuator [111]. For thermo-electric actuators, the driving temperature change can be given by direct Joule heating or by a united heating resistor. Some micro-actuators have been worked in a Si-metal in combination with bimorph cantilever structures. The development of a functional layer in an actuator permits to integrate with uni-morphous/bi-morphous membranes and cantilevers in a micro-system. The deflection based on the relative change in length and making the curvature of the functional layer in a specific design, as shown in Fig. 8 (g) [112].

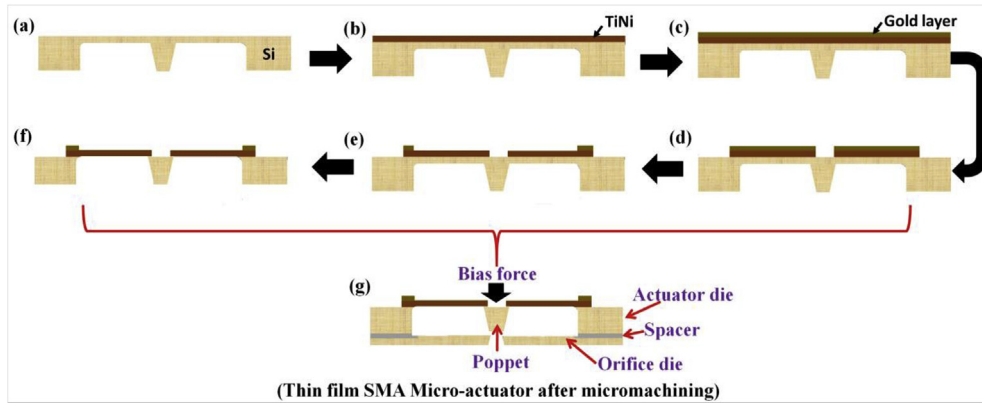


Fig. 8 – Shows the steps of micromachining: (a) forming thin membranes of silicon (~40 μm) (back side) by etching for sputtering, which will be the poppet of the valve, (b) sputter deposition of NiTi (on the front side) followed by annealing; (c) gold sputtering on NiTi which provide electrical contact to conductive path of the actuator; (d) patterning and wet etching of the gold and NiTi film; (e) removing the gold from the active parts of the actuators. Gold remains only on the contact tabs and interconnecting parts of the NiTi; (f) final backside etching for releasing the poppet and active parts of the actuator; and (g) assembled micro valve.

13.2. Micro-pumps and micro-valves

NiTi thin films based MEMS micro-pumps and micro-valves are suitable for a wide range of area such as analytical instruments, implantable drug delivery, chemical analysis, etc. variety of NiTi thin film designs are available, but mostly NiTi-membrane or diaphragm type is chosen for actuation purpose [113–115]. Both freestanding as well as constrained NiTi thin films are used in industrial applications. Although free-standing NiTi thin film has built-in two-way SME, in accordance with maximizing this effect, extra techniques, such as externally biased structure (such as a polyimide layer [4], or a bonded Si cap [116], or glass cap [117]) and 3-D hot-shaping of

Ni–Ti film (membrane) have often been used. Micro-pumps and micro-valves with Ni–Ti/Si bimorph membrane are as the driver diaphragm includes [118]: (i) larger force in their actuation; (ii) coherency in process and no other bias structure needed because Si-substrate can give the bias force; and (iii) no separate structure is required because Si structure can separate the working liquid from SMA thin film completely.

Micro-propulsion that achieves a low leak rate in space applications uses some SMA microvalve. Details of the NiTi Alloy components which are used to produces the commercially accessible micro-valve is represented in Fig. 10 [16]. It composed of an actuator die, a poppet having 3.5 μm thick, and 250 μm wide (Fig. 10b), a Si orifice dies, a bias spring, and a

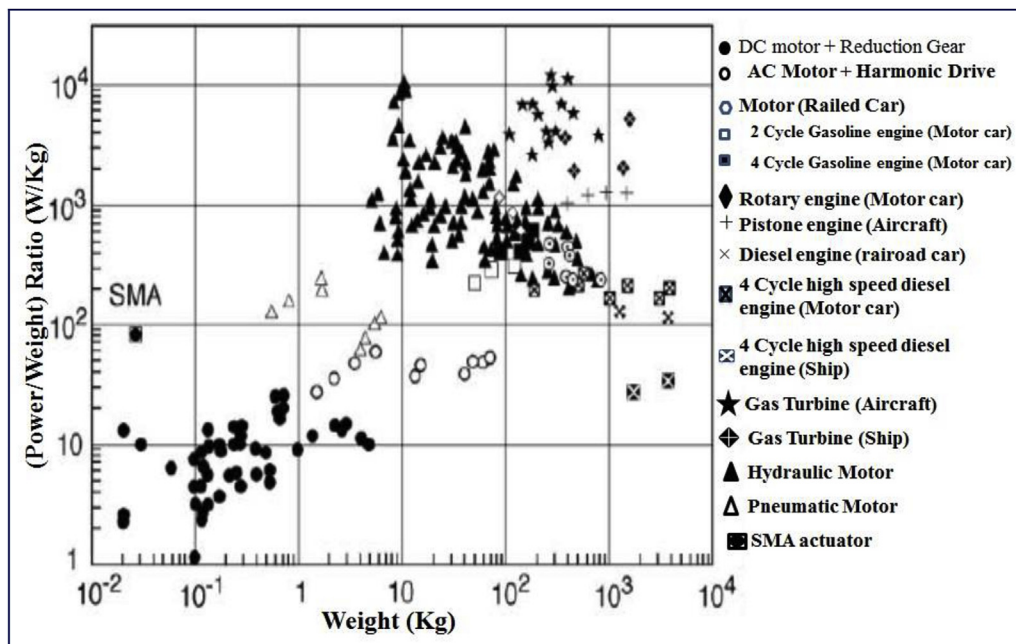


Fig. 9 – Power weight ratio vs. weight diagram of the actuator [110].

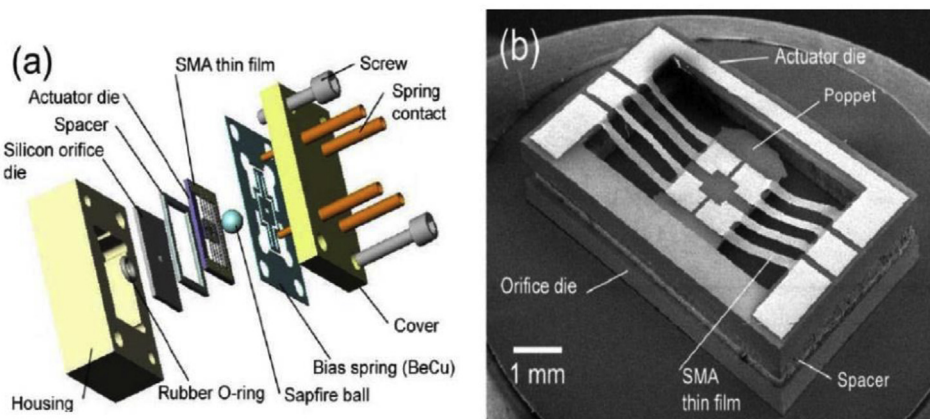


Fig. 10 – Micro-valve (a) assembled parts showing use of SMA thin film, and (b) micro-machined assemble system [16].

spacer. All elements are assembled in a plastic package (Fig. 10a). The poppet forced by the bias spring in the direction of the orifice, the thin film that supported on the poppet undergoes a phase transformation from martensite to austenite by resistive heating. The original length of NiTi-strip recovered in the phase transformation, and again the poppet lifted by the bias force results in the unlocking of the valve. This device is working with 50–100 mA electric current and 0.5 N bias forces causes, ~100 μm displacement of the poppet with ~10 ms response time and 2000 sccm maximum flow at 1.3 atm.

### 13.3. Micro-grippers

Holding and operating a tiny object with more accuracy is essential for many precise applications like ‘assembly in micro-systems’, ‘drug delivery micromanipulators for cells’, and ‘endoscopes for microsurgery’. Micro-grippers help to enable more accessible work like opening the distance for assembling work, gripping force, etc. The complete size of the micro-wrapper arms is nearly 100 μm which is nearly equal to a human hair diameter. Among two different design of micro-gripper (in-plane and out-of-plane bending mode), the out-of-

plane bending mode is well liked in which two integrated NiTi/Si cantilevers are worked with opposite actuation directions (Fig. 11a) [119,120]. Fig. 11b gives the top view of NiTi electrodes patterned on Si cantilevers. The SMA NiTi thin film cantilever bends up as soon as get the heat and generate a gripping force. Generally, these gripper designs are used to unite different cantilevers to generate large force as well as displacement.

A freestanding NiTi thin film without out-of-plane movement is given in Fig. 12[121]. The arms of the micro-wrapper maintain it’s in a flat shape as long as the current through it and by the withdrawal of the current, the arms bend to form a coupling agent. These devices are used to operate the micro-organisms and to detach abnormalities such as tumours inside the body. A novel microelectrode with NiTi clipping structure has been studied by Fu et al [122]., which is used to clip a nerve cord or other living organisms. The NiTi thin film SMA is activating application of the current which gives a clipping force to the electrode to clip the nerve as shown in Fig. 13a and b. In the in-plane bending mode, the actuation of the two film arms are within a plane comprehend by cooperative structure design [108]. A micro-tweezer structure studied by Fu et al., [123]., in which residual stress act as a bias

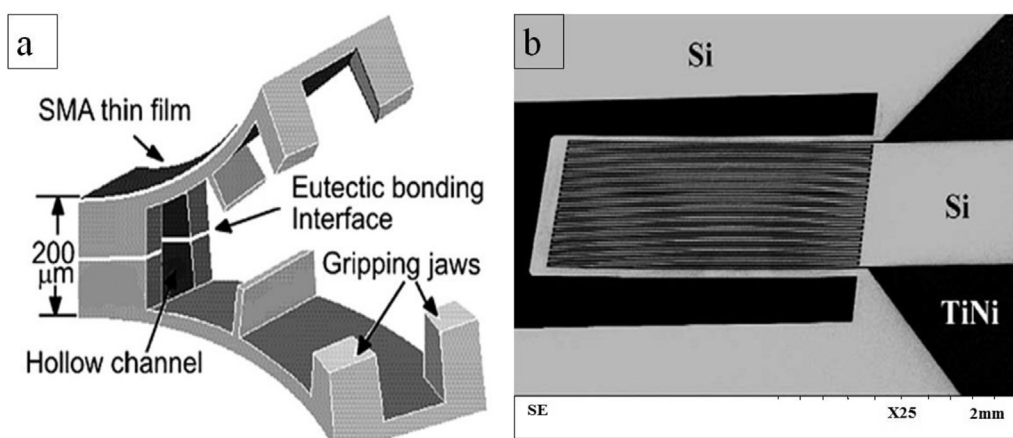
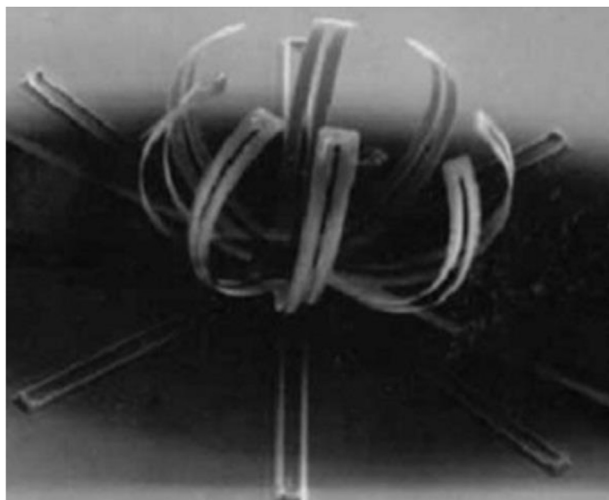


Fig. 11 – NiTi/Si micro-gripper with out-of-plane bending mode cantilever: (a) micro-gripper, (b) top view of Ni–Ti electrodes patterned on Si cantilevers.



**Fig. 12 – The freestanding NiTi films micro-wrapper (shown in the resolution of 200  $\mu\text{m}$ ) [129].**

force. This can obliterate the requirement of bias force for device action.

#### 13.4. Micro-sensors, micro-switches, and micro-relays

NiTi thin films are very sensitive to surrounding stimulus like the thermal field, electrical fields, magnetic field, stress, etc. that leads the application in micro-sensor. Other applications are switches or micro-relays, fiber optics switching, automotive fuel injectors, automatic probe tips in test equipment, micro-lens positioner, etc. The surface roughness and refractive index indicate about the phase transformation of NiTi film [10,124]. Austenite phase has a higher reflection coefficient than martensite phase by more than 45%. Due to this type of behaviour in NiTi thin film is used in the valve or on-off optical switch for spatial light modulators [125]. In optical switch lenses, the NiTi thin film helps to displace the optical lens up or down (not left or right), acting as an out-of-plane micro-actuator. In field emission flat panel display, the NiTi thin film based micro-actuators can put together and set

upright a large number of micromachined spacers between the pixels [126].

In Far-infrared-radiation imaging sensor one side of the NiTi film cantilever is deposited with an infrared absorbing layer, and another side is deposited with a gold reflecting layer. By absorbing the infrared radiation, the temperature of NiTi cantilever changes that results in a large tilting effect and realizing the illumination of gold reflective layer [127]. Fig. 14 depicts a NiTi/Si beam micro-mirror structure embedded with a top Si mirror cap, and different arms are used to actuating the Si cap by applying Joule heating. The limitation of this device is with the Si which cannot be deformed greater than 1–3% strain.

#### 13.5. Anti-vibration damping structures

Anti-vibration damping structures are highly depending on the martensitic transformation temperature and frequency. The pseudoelasticity behaviour of NiTi thin film plays a dominant role to reduce the vibrations during their work. The positioning accuracy of the read/writes heads in hard disk drives strongly depends on the inherent vibration characteristics of the head actuator assembly. The NiTi thin film is the main material to reduce the vibration in the hard disk drive [128].

#### 13.6. Super mirror application

NiTi thin film spreads a special attraction in the field of super mirror fabrication. Smooth surface layering and homogenized interface are essential for neutron super mirror applications [129,130]. A multilayered mirror design can refine the intensity of reflection of polarized neutrons at a lower angle (grazing incidence angle) in comparison to traditional Ni-mirrors. A commercial Ni/Ti multilayer mirror made up of 15–20 layers of the pair (Ni and Ti layer) which are of 25–30 nm thick.

#### 13.7. Aero-microelectromechanical systems

Thin film MEMS-activated devices are positioned under the aerodynamic skin. The traveling wave produced by the

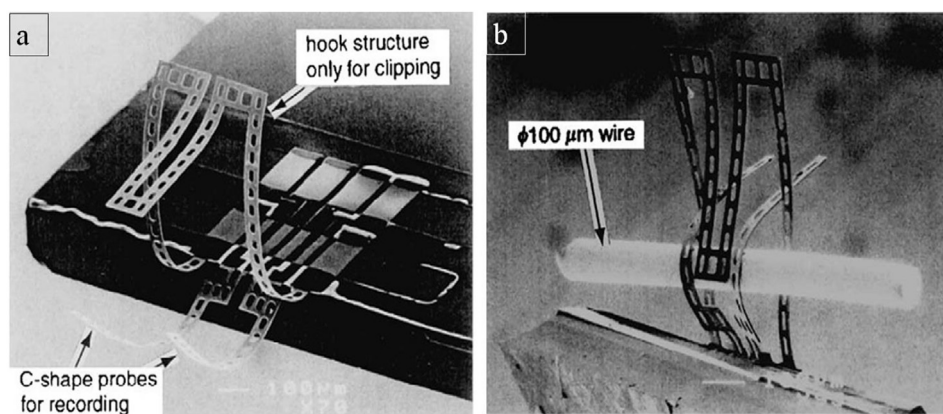


**Fig. 13 – (a) A NiTi electrodes with the hook structure is returned to its memorized shape when it is heated, while two C-shape probes for recording are not heated; (b) the microelectrode clipping a wire (100  $\mu\text{m}$ ) after the hook structure is heated [130].**

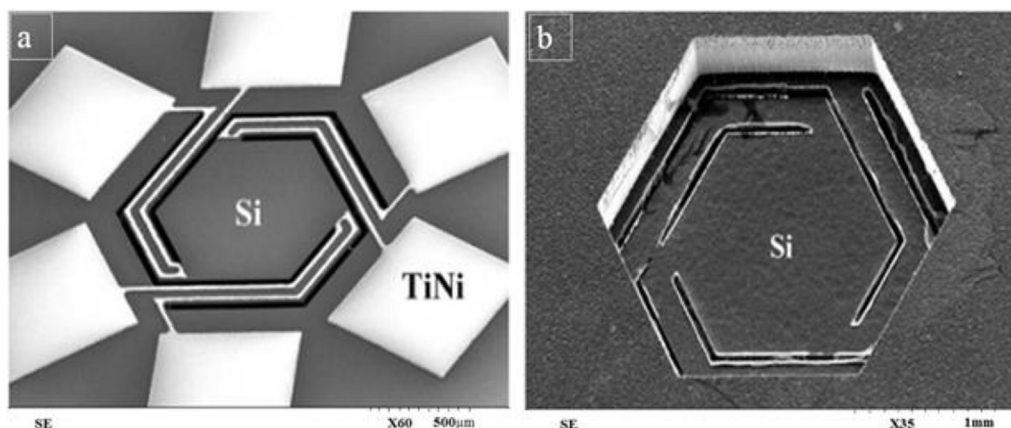


**Fig. 14** – NiTi micro-mirror structure with a top mirror Si cap and the arms fabricated with NiTi/Si beam structure: (a) top view, (b) bottom view.

different device in the skin help to energize the boundary layer and thus decrease the turbulent drag. The shape memory alloy component with their standard size gives the low actuation frequencies; therefore a sufficient number of shape memory alloy thin film components have demonstrated 30 Hz actuation frequencies [131,132].

#### 14. Limitation of shape memory alloy

In spite of exceptional behaviour, full assimilation of SMA thin films into micro-electro-mechanical-system is limited. Their stoichiometry responsiveness has major limitation for the reliability and manufacturability of these materials in MEMS [133,134]. Further, the application of NiTi SMAs in MEMS has been obstructed by different fabrication factors such as:

- The economic batch fabrication of NiTi films with reproducible transformation temperatures and transformation strains [19].
- The large exothermic heat of transformation that limits the cycle lifetime, as well as poor machinability that limits its ability to be used in many applications [135].
- Have low energy efficiency, lower in the speed of dynamic response and larger hysteresis temperature [4].
- Non-linearity and complex thermomechanical property and ineffectiveness of accurate and complex motion control [4].
- Higher in the cost of NiTi thin films and problems in self-control of the composition as well as the related mechanical behaviour.
- The existence of fatigue problems and potential degradation [4].
- As-deposited sputtered thin films are amorphous, and an annealing step (>500 °C) is required for crystallization [136].

#### 15. Conclusion and summary

SMA possess numerous valuable properties, which permits creating novel functional materials. Thin film shape memory actuators are transformative products used in micro-systems and well integrated within miniaturized system. Their reduced size; around microns; together with processing route enable microsystem fabrication processes to be used successfully in sensors, actuators and electronics control units. The SME and PE properties produced through sputtering of NiTi thin films depends on different sputtering parameters (target power, gas pressure, substrate-to-target distance, substrate bias, deposition temperature, deposition environment etc.), metallurgical factors (alloy composition, annealing, aging, thermo-mechanical treatment etc.) and the application conditions (working temperature, loading conditions, heating/cooling rate, etc.). The substrate used to growth of the thin film play a major role in preferred orientation, adhesion and chemical interaction of the NiTi thin films. The intermetallic formed through NiTi system increases the wear properties as well as mechanical properties of the thin film. The substitution of the third element in the near equiatomic NiTi alloys allows better SME characteristics which directly affects its transformation behaviour (one-stage transforms to two-stage). Superior yield stress, good fracture resistance and an appropriate ductility enable NiTi thin film very attractive for most practical applications. Application of SMAs is commonly found in two major engineering direction; one is SME for actuation usage and other is PE used for vibration resistance and dampening. The SMA-materials are integrated in micro-electro-mechanical devices cause their design flexibility, produce a clean working environment, work with friction-free and non-vibration movement. The combination of superelasticity performances and their mechanical ability prove to be key to success in miniaturization of the systems.

## Declaration of Competing Interest

The authors declare that they have no known competing financial interests or personal relationships that could have appeared to influence the work reported in this paper.

## REFERENCES

- [1] Sadighi A, Kim W. *IEEE/ASME Trans Mechatron* 2011;16:371–9.
- [2] Haddad YM. *Mech Behav Eng Mater* 2000;404–21. ISBN: 978-94-017-2231-5.
- [3] Sanjabi S, Naderi M, ZareBidaki H, Sadrnezhaad SK. *Trans. B: Mech Eng* 2009;16:248–52.
- [4] Fu Y, Du H, Huang W, Zhang S, Hu M. *Sens Actuators, A* 2004;112:395–408.
- [5] He Q, Huang WM, Hong MH, Wu MJ, Fu YQ, Chong TC, Chellet F, Du HJ. *Smart Mater Struct* 2004;13:977–82.
- [6] Readey DW. *Kinetics in materials science and engineering*. CRC Press; 2017. p. 223. ISBN: 9781482235678.
- [7] Ho KK, Carman GP. *Thin Solid Films* 2000;370:18–29.
- [8] Rao J, Roberts T, Lawson K, Nicholls J. *Surf Coating Technol* 2010;204:2331–6.
- [9] Ziolkowski A, Heinemann B. *Pseudoelasticity of shape memory alloys: theory and experimental studies*. 2015. p. 17. ISBN: 9780128018019.
- [10] Otsuka K, Ren X. *Prog Mater Sci* 2005;50:511–678.
- [11] EswarRaju KSS, Bysakh S, Sumesh MA, Kamat SV, Mohan S. *Mater Sci Eng, A* 2008;476:267–73.
- [12] Lai BK, Hahm G, You L, Shih CL, Kahn H, Phillips SM, Heuer AH. *Mat. Res. Soc. Symp.Proc.vol. 657*. Materials Research Society; 2001. EE8.3.1–EE8.3.6.
- [13] Bifano TG, Johnson HT, Bierden P, Mali RK. *J Microelectromech Syst* 2002;11:592–7.
- [14] Quandt E, Holleck H. *Microsyst Technol* 1995;4:178–84.
- [15] Winzek B, Schmitz S, Rumpf H, Sterzl T, Hassdorf R, Thienhaus S, Feydt J, Moske M, Quandt E. *Mater Sci Eng, A* 2004;378:40–6.
- [16] Ishida A, Martynov V. *MRS Bull* 2002;27:111–4.
- [17] Variola F, Brunski JB, Orsini G, Tambasco d Oliveira P, Wazen R, Nanci A. *Nanoscale* 2011;3: 335–35.
- [18] Feninat FE, Laroche G, Fiset M, Mantovani D. *Adv Eng Mater* 2002;4:91–104.
- [19] Shih CL, Lai BK, Kahn H, Philips SM, Heuer AH. *J Microelectromech Syst* 2001;10:69–79.
- [20] Fu Y, Huang W, Du H, Huang X, Tan J, Gao X. *Surf Coating Technol* 2001;145:107–12.
- [21] Miyazaki S, Qing Fu Y, Huan WM. *Thin Film Shape Memory Alloys: Fundamentals and Device Applications*. 2009. ISBN: 978-0-521-88576-8.
- [22] Fu YQ, Du HJ. *Surf Coat Technol* 2002;153/1:100–5.
- [23] Fu YQ, Du HJ. *Mater Sci Eng, A* 2003;339:10–6.
- [24] M Craciunescu C, Mihalca I, Budau V. *J Optoelectron Adv Mater* 2005;7:1113–20.
- [25] Zhang JX, Sato M, Ishida A. *Acta Mater* 2001;49:3001–10.
- [26] Fu YQ, Luo JK, Huang WM, Flewitt AJ, Milne WI. *J Phys Conf* 2007;76:12032. <https://doi.org/10.1088/1742-6596/76/1/012032>.
- [27] Greiner C, Oppenheimer SM, Dunand DC. *Acta Biomater* 2005;1:705–16.
- [28] Heller L, Vokoun D, Sittner P, Finckh H. *Smart Mater Struct* 2012;21:45016. <https://doi.org/10.1088/0964-1726/21/4/045016>.
- [29] Tomozawa M, Okutsu K, Kim HY, Miyazaki S. *Mater Sci Forum* 2005;475–479:2037–42.
- [30] Bertheville B. *Mater Trans* 2006;47:698–703.
- [31] Martins RMS, Schell N, Silva RJC, Pereira L, Mahesh KK, Fernandes FMB. *Sens Actuators, B* 2007;126:332–7.
- [32] Sanjabi S, Sadrnezhaad SK, Yates KA, Barber ZH. *Thin Solid Films* 2005;491:190.
- [33] Sanjabi S, Barber ZH. *Surf Coating Technol* 2010;204:1299–304.
- [34] Abhilash V, Sumesh MA, Mohan S. *Smart Mater Struct* 2005;14:S323–8.
- [35] Fu Y, Du H, Zhang S. *Surf Coating Technol* 2003;167:129–36.
- [36] Hahm G, Kahn H, Phillips SM, Heuer AH. *Fully microfabricated, solid-state sensor and actuator workshop hi/ton head Island*. 2000. p. 230–3. South Carolina.
- [37] Chu PK. *Surf Coating Technol* 2007;201:8076–82.
- [38] Qiao Z. *Fabrication and study of ito thin films prepared by magnetron sputtering (Dissertation)*. zurErlangung des Grade; 2003. p. 1–146.
- [39] Harper JME, Berg S, Nender C, Katardjiev IV, Motakef S. *J Vac Sci Technol* 1992;10:1765.
- [40] Ho KK, Mohanchandra KP, Carman GP. *Thin Solid Films* 2002;413:1.
- [41] Alin SH. *Electrical studies of silicon and low K dielectric materials (Thesis)*. Massachusetts Institute of Technology; 1999.
- [42] Chu a JP, Lai YW, Lin TN, Wang SF. *Mater Sci Eng, A* 2000;277:11–7.
- [43] Chu JP, Chung CH, Lee PY, Rigsbee JM, Wang JY. *Metall Mater Trans, A* 1998;29A:647.
- [44] Doliquea V, Thomanna AL, Braulta P, Tessiera Y, Gillon P. *Mater Chem Phys* 2009;117:142–7.
- [45] Segal V, Thomas M, Li J, Ferrasse S, Alford F, Scott T, Turner S. *Fine grain size material, sputtering target, methods of forming, and micro-arc reduction method*. Publication number: US20030052000 A1. 2003.
- [46] Chen T, Wong M, Shun T, Yeh J. *Surf Coating Technol* 2005;200:1361–5.
- [47] Quandt E, Halene C, Holleck H, Feit K, Kohl M, Smacher PS, Skokan A, Skrobaneck KD. *Sens Actuators A* 1996;53:434–9.
- [48] Locci AM, Orru R, Cao G, Munir ZA. *Intermetallics* 2003;11:555–71.
- [49] Adharapurapu, Raghavendra R, UC san Diego electronic theses and Dissertations, University of California (2007).
- [50] Fernandes FMB, Mahesh KK, Paula AS. *Thermomechanical treatments for Ni-Ti alloys*. In: *Shape memory alloys-processing, characterization and applications*; 2013. p. 1–26.
- [51] Duerig T, Pelton A, Trepanier C. *Nitinol, CHAPTER 9: alloying and composition*. ASM International; 2011.
- [52] Goryczka T, Morawiec H. *J Alloys Compd* 2004;367:137–41.
- [53] Zhang W, Hackl K. *Mater Trans* 2006;47:720–3.
- [54] ichiSaitoh K, Sato T, Shinke N. *Mater Trans* 2006;47:742–9.
- [55] Sakurai J, Hosoda H, Miyazaki S. *Mater Sci Forum* 2000;327–328:175–8.
- [56] Wan D, Komvopoulos K. *J Mater Res* 2005;20:6. <https://doi.org/10.1557/JMR.2005.0209>.
- [57] Miyazaki S, Otsuka K. *ISIJ Int* 1989;29:353–77.
- [58] Gabry B, Lexcelent C, Nob VH, Miyazaki S. *Thin Solid Films* 2000;372:118–33.
- [59] Martins RMS, Brazfernandes FM, Silva RJC, Pereira L, Gordo PR, Maneira MJP, Beckers M, Ucklich AM, Schell N. *Appl Phys A* 2006;83:139–45.
- [60] Miyazaki S, Ishida A. *Mater Sci Eng, A* 1999;273–275:106–33.
- [61] Wei ZG, Sandstrom R, Miyazaki S. *J MaterSci* 1998;33:3743–62.
- [62] Ishida A, Sato M, Kimura T, Sawaguchi T. *Mater Trans* 2001;42:1060.

- [63] Kajiwaru S, Ogawa K, Kikuchi T, Matsunaga T, Miyazaki S. *Phil Mag Lett* 1996;74:395–404.
- [64] Zarnetta R, Konig D, Zamponi C, Aghajani A, Frenzel J, Eggeler G, Ludwig A. *Acta Mater* 2009;57:4169–77.
- [65] Wang FE. *Bonding theory for metals and alloys*. ISBN: 044451978-5. Library of congress cataloguing in publishing data; 2005.
- [66] Srivastava AK, Schryvers D, Humbeeck JV. *Intermetallics* 2007;15. 1538e1547.
- [67] Satoh G, Birnbaum A, Yao YL. *J Manuf Sci Eng* 2010;132:51004–9.
- [68] Nurveren K, Akdogan A, Huang WM. *J Mater Process Technol* 2008;196:129–34.
- [69] Otsuka K, Wayman CM. *Shape memory materials*, vol. 284. Cambridge University Press; 1999. ISBN: 978052166384.
- [70] Saburi T, Ncnno S, Fukuda T. *J Less Common Met* 1986;125:157.
- [71] Yeh CL, Sung WY. *J Alloys Compd* 2004;376:79–88.
- [72] Ohta A, Bhansali S, Kishimoto I, Umeda A. *Sens Actuators* 2000;8:165–70.
- [73] Tao A. *Preparation and characterization of TiN/SiNx nanolayered films and their fracture behaviour (Thesis)*. 2008.
- [74] Janssen GCAM. *Thin Solid Films* 2007;515:6654–64.
- [75] Priyadarshini GB. *Titanium and nickel-titanium thin films by magnetron sputtering: influence of process parameters (Thesis)*. Department of Metallurgical and Materials Engineering Indian Institute of Technology Kharagpur; 2011.
- [76] Behera A, Aich S. *Surf Interface Anal* 2015;47:805–14.
- [77] Shabalovskayaa S, Anderegg J, Van Humbeeck J. *Acta Biomater* 2008;4:47–467.
- [78] Matsunaga T, Kajiwaru S, Ogawa K, Kikuchi T, Miyazaki S. *Acta Mater* 2001;49:1921–8.
- [79] Shaw GA, Crone WC, Wi M. *Materials research society. Mater Res Soc Symp Proc* 2004;791.
- [80] Ikuta K, Fujishiro H, Hayashi M, Matsuura T. In: *Asilomar Conference Center, Pacific Grove, California, USA*; 1994. p. 13.
- [81] Mandepud SK. *Engineering the stress temperature response of shape memory alloy thin films through the development of composite structures*. 2008. p. 150. ISBN: 9780549589532.
- [82] Kajiwaru S. *J Phys* 2001;11. <https://doi.org/10.1051/jp4:2001866>. Pr8-395-Pr8-405.
- [83] Martins RMS, Schell N, Silva RJC, Fernandes FMB. *Nucl Instrum Methods Phys Res, Sect B* 2005;238:319–22.
- [84] Tan L, Crone WC, Sridharan K. *J Mater Sci Mater Med* 2002;13:501–8.
- [85] Chua CL, Chung CY, Lin PH, Wang SD. *Mater Sci Eng, A* 2004;366:114–9.
- [86] Latrice N, Odum H. *The characterization of thin film Nickel-Titanium shape memory alloys, Auburn, Alabama (Thesis)*. 2010.
- [87] Behera A, Aich S, Ghosh S. *Emerg Mater Res* 2017;6:1–6.
- [88] Behera A, Suman R, Aich S, Mohapatra SS. *Surf Interface Anal* 2016;49:620–9.
- [89] Fu Y, Du H, Zhang S. *Mater Lett* 2003;57:2995–9.
- [90] Maitz MF. *Surface modification of Ti-Ni alloys for biomedical applications, Shape memory alloys for biomedical applications*. In: Yoneyama Takayuki, Miyazaki Shuichi, editors. Woodhead Publishing; 2008. p. 173–93. ISBN 978-1-84569-524-8.
- [91] Grummon DS, Gotthardt R. *Acta Mater* 2000;48:635–46.
- [92] Lagrange TB, Gotthardt R. *J Optoelectron Adv Mater* 2003;5:313–8.
- [93] Craciunescu C, Wuttig M. *Thin Solid Films* 2000;379:173–5.
- [94] Lehnert T, Tixier S, Boni P, Gotthardt R. *Mater Sci Eng, A* 1999;273–275:713–6.
- [95] Shao AL, Cheng Y, Zhou Y, Li M, Xi TF, Zheng YF, Wei SC, Zhang DY. *J Coating Technol* 2013;228:S257–61.
- [96] Spiga D, Pareschi G, Cotroneo V, Canestrari R, Vernani D. *Opt Eng* 2007;46:8. 086501.
- [97] Boudou T, Crouzier T, Ren K, Blin G, Picart C. *Adv Mater* 2009;21:1–27.
- [98] Goryczka T, Dudek K, Szaraniec B, Lełątko J. *GornictwoInżynieria Materiałowa* 2013:4.
- [99] Padiyath JK. *Analysis of sputtered multilayers and design of a neutron monochromator (Thesis)*. Swiss Federal Institute of Technology Zurich; 2006.
- [100] Krogman KC, Zacharia NS, Schroeder S, Hammond PT. *Langmuir* 2007;23:3137–41.
- [101] Fuentes JMG, Gumpel P, Strittmatter J. *Adv Eng Mater* 2002;4:437–51.
- [102] Krogman KC, Lowery JL, Zacharia NS, Hammond PT. *Nat Mater* 2009;8:512–8.
- [103] Merrill MH, Sun CT. *Nanotechnology* 2009;20:1–6.
- [104] Gittleston FS, Kohn DJ, Li X, Taylor AD. *ACS Nano* 2012;6:3703–11.
- [105] Tomozawa M, Kim HY, Miyazaki S. *J IntellMater Syst Struct* 2006;17:1049–58.
- [106] Fischer AC, Gradin H, Braun S, Schröder S, Stemme G, Niklaus F. *Micro electro mechanical Syst*. 2011. p. 348–51.
- [107] Walker JA, Mehregany M, Gabriel KJ. *Sens Actuators, A* 1990;21–23:243.
- [108] Fu Y, Du H, Zhang S, Ong S. *Thin Solid Films* 2005;476:352.
- [109] Wang RX, Zohar Y, Wong M. *J Micromech Microeng* 2002;12:323.
- [110] Ikuta K. In: *Proc. IEEE Int. Conf. on Robotics and Automation-90, Cincinnati*. Cincinnati: The Institute of Electrical and Electronics Engineers, Inc.; 1990. p. 2156.
- [111] Degeratu S, Rotaru P, Manolea G, Manolea HO, Rotaru A. *J Therm Anal Calorim* 2009;97:695–700.
- [112] Lee CJ. *International mechanical engineering congress and exposition dynamic systems and control New Orleans, Louisiana, USA, Conference Sponsors: dynamic systems and control division*. ISBN: 0-7918-3629-0. 2002.
- [113] Nisar A, Afzulpurkar Nitin, Mahaisavariya Banchoong, Tuantranont Adisorn. *Sens Actuators, B* 2008;130:917–42.
- [114] Zhang C, Xing D, Li Y. *Biotechnol Adv* 2007;25:483–514.
- [115] Makino E, Mitsuya T, Shibata T. *Sens. Actuators* 2000;79:128–35.
- [116] Makino E, Mitsuya T, Shibata T. *Sens Actuators A* 2000;79:251–9.
- [117] Makino E, Mitsuya T, Shibata T. *Sens Actuators A* 2001;88:256–62.
- [118] Xu D, Wang L, Ding GF, Zhou Y, Yu AB, Cai BC. *Sens Actuators A* 2001;93:87–92.
- [119] Bellouard Y. *Mater Sci Eng, A* 2008;481–482:582–9.
- [120] Gill JJ, Chang DT, Momoda LA, Carman GP. *Sens Actuators A* 2001;93:148.
- [121] Takeuchi S, Shimoyama I. *Micro Electro Mech Syst* 2000;9:24–31.
- [122] Fu YQ, Du HJ. *Smart sensors, actuators, and MEMS, 19-21, gran Canaria, Spain, SPIE-Int. Soc. Opt. Eng, USA, vol. 5116, SPIE*; 2003. p. 38–47.
- [123] Fu YQ, Luo JK, Flewitt AJ, Huang WM, Zhang S, Du HJ, Milne WI. *Int J Comput Mater Sci Surf Eng* 2009;2:208–26.
- [124] Sreekumar M, Nagarajan T, Singaperumal M, Zoppi M, Molino R. *Ind Robot: Int J* 2007;34:285–94.
- [125] Chiao J, Hariz AJ, Jamieson DN, Parish G, Varadan VK. In: *Proceedings of SPIE, vol. 5276*; 2004. p. 600. ISBN: 9780819451699.

- [126] Fu YQ, Luo JK, Flewitt AJ, Huang WM, Zhang S, Du HJ, Milne WI. *Int J Nanomanufact* 2020;1–19. Inderscience Enterprises Ltd, [http://www.researchgate.net/publication/228627890\\_Thin\\_film\\_shape\\_memory\\_alloys\\_and\\_microactuators/file/60b7d514f1268589b0.pdf](http://www.researchgate.net/publication/228627890_Thin_film_shape_memory_alloys_and_microactuators/file/60b7d514f1268589b0.pdf).
- [127] Boisen A, Dohn S, Sylvest Keller S, Schmid S, Tenje M. *Rep Prog Phys* 2011;74:1–30.
- [128] Han Y, Li QS, Li A, Leung AYT, Lin P. *Earthq Eng Struct Dynam* 2003;32:483–94.
- [129] Rehm C, Agamalian M. *Appl Phys A* 2002;74:s1483–5.
- [130] Zhong Z, Zhan-Shan W, Jing-Tao Z, Feng-Li W, Yong-Rong W, Shu-Ji Q, Ling-Yan C. *Chinese Phys. Lett.* 2006;23:2678.
- [131] Mani R, Lagoudas D, Rediniotis O. *Smart Struct Mater* 2003;5056. San Diego, CA.
- [132] Gill J, Ho K, Carman G. *J Microelectromechan Syst* 2002;11:68–77.
- [133] Forsberg F. Thesis: Heterogeneous material integration for MEMS. 2013. p. 1–87. 039, <http://urn.kb.se/resolve?urn=urn:nbn:se:kth:diva-129185>.
- [134] Vilarinho PM. *Functional materials: properties, processing and applications; scanning probe microscopy: characterization, nanofabrication and device application of functional materials*, NATO science series II: mathematics. *Phys Chem* 2005;186:3–33. ISBN: 978-1-4020-3019-2.
- [135] Patoor E, Lagoudas DC, Entchev PB, Brinson LC, Gao X. *Mech Mater* 2006;38:391–429.
- [136] Lee H, Ramirez AG. *Appl Phys Lett* 2004;85:716.

Dr. Catalin Pruncu is a Researcher Fellow in the Department of Mechanical Engineering at Imperial College London, UK with 10 years of research experience in academia and industry. I have published about 70 papers in ISI journals, 2 books, a patent and other papers at various national and international conferences. Recently I was invited as Editor for “Special Issue” *Wear Behavior of Polymer Composites*, MDPI “and I am reviewer for almost 35 ISI journals including “Measurement, Elsevier”, “Journal of Materials Research and Technology”, “Surface and Coatings Technology”, “Journal of Cleaner Production” and etc. I am also an organizing or scientific member in various national and international conferences, including “The International Conference on Advanced Composite Materials Engineering (COMAT)” Brasov, Romania.